Optimum Receiver Design for Wireless Broad-Band Systems Using OFDM—Part I

Michael Speth, *Student Member, IEEE,* Stefan A. Fechtel, *Member, IEEE,* Gunnar Fock, and Heinrich Meyr, *Fellow, IEEE*

Abstract— Orthogonal frequency-division multiplexing (OFDM) is the technique of choice in digital broad-band applications that must cope with highly dispersive transmission media at low receiver implementation cost. In this paper, we focus on the inner OFDM receiver and its functions necessary to demodulate the received signal and deliver soft information to the outer receiver for decoding. In Part I of this paper, the effects of relevant nonideal transmission conditions are thoroughly analyzed: imperfect channel estimation, symbol frame offset, carrier and sampling clock frequency offset, time-selective fading, and critical analog components. Through an appropriate optimization criterion (signal-to-noise ratio loss), minimum requirements on each receiver synchronization function are systematically derived. An equivalent signal model encompassing the effects of all relevant imperfections is then formulated in a generalized framework. Part I concludes with an outline of synchronization strategies to be detailed in Part II.

Index Terms—OFDM, receiver design, synchronization.

I. INTRODUCTION

THE MODULATION scheme orthogonal frequency-division multiplexing (OFDM), chosen for the two European terrestrial broadcasting standards—digital audio broadcasting (DAB) and digital video broadcasting (DVB-T) [2], [3], is now considered a mature and well-established technology for digital broadcasting applications. Thanks to its virtues, it is currently under investigation for further broad-band applications such as wireless asynchronous transfer mode and wireless networks [4]. For an introduction into the basics of OFDM, refer to [5] and [6].

The main advantage of OFDM is that it allows transmission over highly frequency-selective channels at a low receiver implementation cost. In particular, costly equalizers needed in single-carrier systems are dramatically simplified or even obsolete in the case that differential modulation schemes are used [7].

A well-known problem of OFDM is its vulnerability to synchronization errors. Many publications have therefore been concerned with this topic. Nevertheless, two questions remain.

1) How much of the theoretical performance of OFDM can be actually realized, taking into account *all* receiver components?
2) How much of the implementation benefits remain when taking into account the *complexity* of algorithms needed for synchronization?

This paper is divided into two parts. In the first part, we thoroughly analyze the impact of receiver imperfections on the system performance and show how receiver components can be optimized in a systematic manner. In the second part, we demonstrate the optimization methodology for the example of a receiver based on the European digital terrestrial TV standard DVB-T and analyze the achievable performance as well as the resulting complexity.

One of the major features of OFDM is the possibility to sacrifice some bandwidth (thus optimality) for the benefit of a simple receiver implementation. However, in order to apply the OFDM principle, the following requirements must hold.

- The channel must be *quasi-static* within one symbol duration.
- The channel dispersion must be *limited* in time.
- The analog components must have *near-ideal* characteristics (e.g., linearity).

While it is possible to relax these requirements somewhat and compensate the detrimental effects by appropriate algorithms (see e.g., [8], [9]), such schemes are not considered here since—at least for the relevant case of a large number of subcarriers—they counteract the notion of OFDM being the technique of choice when it comes to implement low-complexity broad-band receivers.

In the receiver design, we follow the principle of synchronized detection [10]. The receiver is divided in an inner and outer part. The transmission parameters—carrier frequency offset, sampling clock offset, timing offset—and the channel are estimated in the inner receiver and then compensated for as if the estimates were the true parameters. The compensated signal is then used to decode the transmitted data in the outer receiver. Of course, the parameter estimates bear some estimation errors, resulting in a performance loss. In order to arrive at the best compromise between the conflicting objectives of minimizing this performance loss and simultaneously minimizing receiver complexity, the following approach is taken.

- A system model comprising all relevant effects of the inner and outer receiver is developed.
- An optimization criterion is formulated that allows to evaluate the quality of each relevant receiver component.

M. Speth, G. Fock, and H. Meyr are with the Institute for Integrated Systems in Signal Processing (ISS), Aachen University of Technology, D-52056 Aachen, Germany (e-mail: speth@ert.rwth-aachen.de; fock@ert.rwth-aachen.de; meyr@ert.rwth-aachen.de).

S. A. Fechtel is with Infineon Technologies AG i.Gr., D81541 München, Germany (e-mail: fechtel@hl.siemens.de).

- Next, the impact of imperfect transmission parameters on the receiver performance is analyzed.
- From this analysis, an equivalent system model at subcarrier level is derived that allows a simplified description of all relevant receiver impairments.

After a short discussion of possible training data formats and their impact on synchronization, we introduce a generalized structure for OFDM receivers. This structure will be the basis for the receiver developed in the second part of this paper.

II. OFDM SIGNAL MODEL

We consider an OFDM system using an inverse fast Fourier transform (IFFT) of size N for modulation. Each OFDM symbol is composed of $K < N$ data symbols $a_{l,k}$, where l denotes the OFDM symbol time index and k denotes the subcarrier frequency index. The output of the IFFT is discrete time with sampling time $T = T_u/N$. In order to limit the transmit signal to a bandwidth smaller than $1/T$ (thus allowing a simple "T-spaced" OFDM receiver), the number K is chosen small enough to provide that so-called "guard bands" at the edges of the transmission spectrum are left free. Using these guard bands, the (periodic) spectrum is limited by using an appropriate analog transmission filter $G_T(\omega)$. The transmitted complex baseband signal can then be described by

$$s(t) = \frac{1}{\sqrt{T_u}} \sum_{l=-\infty}^{+\infty} \sum_{k=-K/2}^{K/2-1} a_{l,k} \psi_{l,k}(t) * g_T(\tau) \quad (1)$$

where $*$ denotes convolution. Each data symbol is shaped by a rectangular pulse of length T_u and modulated onto a subcarrier with (baseband) frequency $f_k = k/T_u$. In order to avoid intersymbol interference (ISI), the OFDM symbol is preceded by a guard interval of length T_g. Taking this into account, the resulting subcarrier pulses are

$$\psi_{l,k}(t) = e^{j2\pi(k/T_u)(t-T_g-lT_s)} u(t - lT_s)$$
$$u(t) = \begin{cases} 1, & 0 \le t < T_s \\ 0, & \text{else.} \end{cases} \quad (2)$$

The resulting symbols are of length $T_s = T_u + T_g$, which is equivalent to $N_s = N + N_g$ samples.

A. Transmission over Frequency-Selective Fading Channels

The signal is transmitted over a frequency selective fading channel

$$h(\tau, t) = \sum_i h_i(t) \cdot \delta(\tau - \tau_i) \quad (3)$$

which is comprised of the actual channel impulse response (CIR) and the transmission filter $g_T(\tau)$. We will further assume that the channel taps are uncorrelated with respect to each other and can be modeled as a wide-sense stationary process where the average energy of the total channel energy is normalized to one, and the delays τ_i are taken to be constant for the time of interest. Assuming the receiver filter is flat within the transmitter bandwidth, the receiver input signal is

$$r(t) = \sum_i h_i(t) \cdot s(t - \tau_i) + n(t). \quad (4)$$

Sampling the signal at time instants $t_n = nT$ yields

$$r(t_n) = \sum_i h_i(nT) \cdot s(nT - \tau_i) + n(nT). \quad (5)$$

After removing the guard interval for further receiver processing, the lth received OFDM symbol is represented by N samples

$$\mathbf{r}_l = \{r_{l,0}, r_{l,1}, \cdots, r_{l,N-2}, r_{l,N-1}\}$$
$$r_{l,n} = r((n + N_g + l \cdot N_s) \cdot T). \quad (6)$$

Demodulation of the subcarriers via a *fast Fourier transform* (FFT) yields the received data symbols

$$z_{l,k} = \sum_{n=0}^{N-1} r_{l,n} \cdot e^{-j2\pi(n/N)k}. \quad (7)$$

For the moment, we assume the channel to be constant during the transmission of one OFDM symbol denoted by $h_i(l)$. The demodulated data symbols (lth OFDM symbol, subcarrier k) can be shown to be given by [11]

$$z_{l,k} = a_{l,k} H_{l,k} + n_{l,k} \quad (8)$$

where $n_{l,k}$ is complex-valued additive white Gaussian noise (AWGN) and

$$H_{l,k} = \sum_i h_i(l) e^{-j2\pi k(\tau_i/T_u)} \quad (9)$$

is the channel transfer function (CTF) at subcarrier frequency $f_k = k/T_u$. Normalizing the average power of data symbols $a_{l,k}$ and the CTF $H_{l,k}$ to one, the average signal-to-noise ratio (SNR) per symbol γ at data subchannel level is given by

$$\gamma = 1/\sigma_N^2$$
$$\sigma_N^2 = E\{|n_{l,k}|^2\} \quad (10)$$

where $E\{\cdots\}$ denotes the expected value.

III. TRANSMISSION OF OFDM SIGNALS

A. Transmission Model

In a real-world passband transmission system, the following parameters cause disturbances in the receiver.

- The sampling time at the receiver T' can no longer be assumed to be identical with the transmitter time T.
- The same holds for the carrier frequency oscillators used for modulating and demodulating the signal. Assuming a small frequency offset relative to the transmission bandwidth, the frequency difference between transmitter and receiver oscillators can be modeled as a time-variant phase offset $\Theta_o(t)$ at the receiver [10].
- The transmitter time scale is unknown to the receiver. Therefore, the receiver OFDM symbol window controlling the removal of the guard interval will usually be offset from its ideal setting by a time εT. This timing delay can equivalently be incorporated into the channel model, resulting in the *effective channel* $h_{\varepsilon,i}$ relevant to the receiver time scale[1]

$$h_\varepsilon(\tau, t) = h(\tau, t) * \delta(\tau - \varepsilon T). \quad (11)$$

---

[1] In the strict sense, $h_\varepsilon(\tau, t) = h(\tau - \varepsilon T, t - \varepsilon T)$, which for small ε is well approximated by (11).
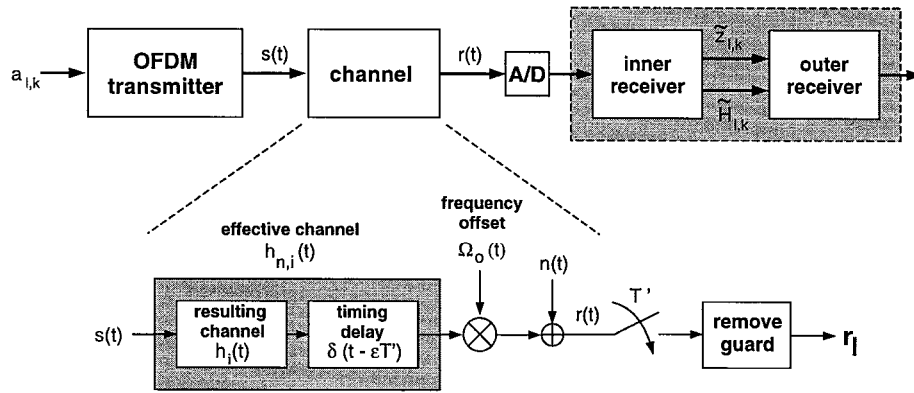
Fig. 1.   Complete baseband transmission model.

All of the effects mentioned are incorporated in the equivalent system model depicted in Fig. 1 [10]. Equation (5) must be modified to yield

$$r(t_n) = e^{j2\pi\Theta_o(nT')} \sum_i h_{\varepsilon,i}(nT') \cdot s(nT' - \tau_i) + n(nT')$$

(12)

and (6) changes to

$$r_{l,n} = r((n + N_g + l \cdot N_s) \cdot T').$$

(13)

This transmission model, comprising all effects caused by the channel and by the inner receiver, is the basis for optimizing the receiver components.

B. Optimization Criterion

In an analogy to [10], the OFDM receiver is divided into an inner receiver and an outer receiver (see Fig. 1). The task of the inner receiver is to provide estimates $\tilde{z}_{l,k}$ and $\tilde{H}_{l,k}$ such that the performance of the outer receiver shows no or minimal degradation compared to a "genius" receiver, which uses the true values $z_{l,k}$ and $H_{l,k}$. An appropriate measure of inner receiver quality is therefore the additional γ ("SNR loss") needed to close the gap between using the estimated ("real") parameters in lieu of the true ("ideal") parameters. We define the SNR loss of the system as

$$\Delta\gamma = \frac{\gamma_{\text{real}}}{\gamma_{\text{ideal}}} = \frac{\sigma_N^{2\,\text{ideal}}}{\sigma_N^{2\,\text{real}}}.$$

(14)

γ_{ideal} denotes the γ required for a certain performance of the outer receiver assuming ideal synchronization, and γ_{real} is the γ required to achieve the same performance with a real receiver. Correspondingly, $\sigma_N^{2\,\text{real}}$ and $\sigma_N^{2\,\text{ideal}}$ denote the noise variances at the inner receiver input that must not be exceeded to achieve a certain outer receiver performance.

In the following section, we discuss the impact of imperfectly estimated parameters on the received signal and on $\Delta\gamma$. As we are primarily interested in the receiver operating under close-to-ideal conditions (steady-state tracking), the analysis is based on a small signal model where a particular parameter of interest is assumed to be the only receiver disturbance, implying that all other parameters are ideal and the channel $h_i(t) = h_i$ is static, except where stated otherwise.

IV. EFFECTS OF NONIDEAL TRANSMISSION CONDITIONS

A. Effects of an Imperfect Channel Estimate

Channel estimation is mandatory if coherent modulation is used. Given a minimum mean square-error channel estimator designed to cope with worst-case channel conditions, the (sub)channel estimate (CTF sample $\tilde{H}_{l,k}$) is well modeled as the true CTF sample $H_{l,k}$ disturbed by AWGN $n_{l,k}^H$

$$\tilde{H}_{l,k} = H_{l,k} + n_{l,k}^H$$

(15)

where the power $\sigma_H^2(\sigma_N^2)$ of the estimation noise $n_{l,k}^H$ is a function of the channel noise variance. The optimum outer receiver features maximum-likelihood (ML) sequence estimation using the signal pair $z_{l,k}$, $\tilde{H}_{l,k}$ delivered by the inner receiver. The resulting performance, given a certain σ_N^2 and σ_H^2, is well approximated by a receiver facing a perfectly known channel and Gaussian noise $n_{l,k}'$ of increased power

$$\sigma_{\text{res}}^2 = \sigma_N^2 + \sigma_H^2(\sigma_N^2).$$

(16)

In order to attain the original receiver performance

$$\sigma_{\text{res}}^2 = \sigma_N^{2\,\text{real}} + \sigma_H^2\left(\sigma_N^{2\,\text{real}}\right)! = \sigma_N^{2\,\text{ideal}}$$

(17)

must hold. From (14) and (17), we can directly derive the loss in performance

$$\Delta\gamma = \frac{\sigma_N^{2\,\text{ideal}}}{\sigma_N^{2\,\text{real}}} = 1 + \frac{\sigma_H^2\left(\sigma_N^{2\,\text{real}}\right)}{\sigma_N^{2\,\text{real}}}.$$

(18)

For the two-dimensional Wiener channel estimator of [12], the estimation noise power is given by

$$\sigma_H^2 = \frac{1}{G}\sigma_N^2$$

(19)

where G is the estimator gain factor, so that the performance loss becomes

$$\Delta\gamma = 1 + \frac{1}{G} = \frac{G+1}{G}.$$

(20)

The factor G results from optimization of the estimator. Its value depends on the number of training data available, the assumed worst-case channel characteristics and the allowable complexity [13].
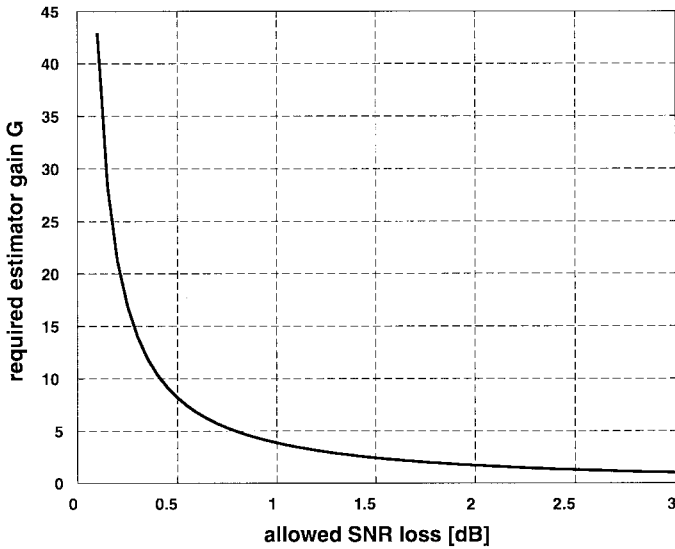
Fig. 2. System loss due to imperfect channel estimation. Required estimator gain G to achieve a given $\Delta\gamma$.

Fig. 2 displays the required estimator gain G versus the allowed system degradation. This result shows the stringent requirement on the quality of the channel estimation. An estimator gain as high as $G = 10$ entails a system loss of 0.41 dB, whereas an allowable loss of 0.1 dB would necessitate an extremely high gain of $G = 43$.

B. Effects of a Symbol (or Frame) Offset

Symbol synchronization in OFDM is closely related to frame synchronization; if symbol timing has been established, frame synchronization follows implicitly. Without loss of generality, we assume a timing offset of $\varepsilon = n_\varepsilon T$ samples (n_ε integer). Changing to the transmitter time scale by using h_i and making the substitution

$$n' = n + n_\varepsilon + N_g + l \cdot N_s \quad (21)$$

the received samples can be expressed as

$$r_{l,n} = \sum_i h_i(t) \cdot s(n'T - \tau_i) + n(n'T). \quad (22)$$

This can be further expanded to yield

$$r_{l,n} = \sum_i h_i(t) \sum_l \sum_k a_{l,k} \cdot \psi(n'T - \tau_i) + n_{l,n}$$

$$\psi(n'T - \tau_i) = e^{j2\pi(k/T_u)(n'T - T_g - lT_s - \tau_i)} u(n'T - lT_s - \tau_i).$$
$$(23)$$

Transmission will be undisturbed if the samples contained in the l_rth *received* OFDM symbol vector $\mathbf{r}_l$ are influenced by the l_rth *transmitted* OFDM symbol *only*. If this is the case, orthogonality between consecutive OFDM symbols will be preserved. This is equivalent to the requirement that for a received OFDM symbol with time index $l_r \neq l$ and all $0 < n < N$, we have

$$u(n'T - lT_s) = u((n + n_\varepsilon + N_g + l_r N_s)T - \tau_i)! = 0. \quad (24)$$

Solving (24) for the preceding symbol ($l = l_r - 1$) and the following symbol ($l = l_r + 1$) yields the range of allowable

timing offsets n_ε

$$\left\lfloor \frac{\tau_{\max}}{T} \right\rfloor - N_g \leq n_\varepsilon \leq 0. \quad (25)$$

Note that no single "correct" synchronization point exists. Depending on the size of maximum channel dispersion $\tau_{\max}$, there may be a large interval of positions n_ε for which the orthogonality of the system is preserved.

In order to understand the effects of a violation of condition (25), it is useful to first analyze the special (but not realistic) case of a nondispersive Gaussian channel ($\tau_{\max} = 0$) and zero guard interval length ($N_g = 0$) so that the range of tolerable positions n_ε reduces to the single point $n_\varepsilon = 0$. Without loss of generality, consider the case $n_\varepsilon > 0$. The vector $\mathbf{r}_l$ now also contains some samples from the symbol $l + 1$

$$\mathbf{r}_l = \{r_{l,n_\varepsilon}, r_{l,n_\varepsilon+1}, \cdots, r_{l,N-1-n_\varepsilon},$$
$$r_{l+1,0}, r_{l+1,1}, \cdots, r_{l+1,n_\varepsilon-1}\}. \quad (26)$$

Demodulation of this vector via the FFT yields

$$z_{l,k} = \frac{N - n_\varepsilon}{N} a_{l,k} e^{j2\pi(k/N)n_\varepsilon}$$

(ICI)
$$+ \frac{1}{N} \sum_{n=0}^{N-1-n_\varepsilon} \sum_{i=-K/2; i\neq k}^{K/2-1} a_{l,i} e^{j2\pi(i/N)(n+n_\varepsilon)}$$
$$\cdot e^{-j2\pi(n/N)k}$$

(ISI)
$$+ \frac{1}{N} \sum_{n=N-n_\varepsilon}^{N-1} \sum_{i=-K/2}^{K/2-1} a_{l+1,i} e^{j2\pi(i/N)(n-N+n_\varepsilon)}$$
$$\cdot e^{-j2\pi(n/N)k} + n_{l,k}. \quad (27)$$

The demodulated signal now consists of a useful portion and disturbances caused by ISI, interchannel interference (ICI), and AWGN. Concerning the useful portion, the transmitted symbols $a_{l,k}$ are attenuated and rotated by a phasor whose phase is proportional to the subcarrier index k and the timing offset n_ε, but they are constant in time. In addition to ISI effects, the demodulated signal suffers from disturbances caused by subcarriers being adjacent to that of the present symbol; orthogonality is no longer preserved so that ICI occurs.

In the presence of a multipath channel, basically the same analysis applies. The post-FFT signal is then described by

$$z_{l,k} = e^{j2\pi(k/N)n_\varepsilon} \alpha(n_\varepsilon) a_{l,k} H_{l,k} + n_{l,k} + n_{n_\varepsilon;l,k} \quad (28)$$

where the ISI and ICI disturbances are modeled as additional noise $n_{n_\varepsilon;l,k}$, and the resulting attenuation of the symbols is well approximated by

$$\alpha(n_\varepsilon) = \sum_i |h_i(t)|^2 \frac{N - \Delta\varepsilon_i}{N}. \quad (29)$$

For OFDM systems with large N, the attenuation $\alpha(n_\varepsilon)$ can usually be neglected. Since the phase rotation is constant in time, it has no impact on systems employing coherent or differential modulation and detection in time direction. Only in the case that differential modulation is used in frequency direction, i.e., across subcarriers (as proposed in [14]), some degradation may result.
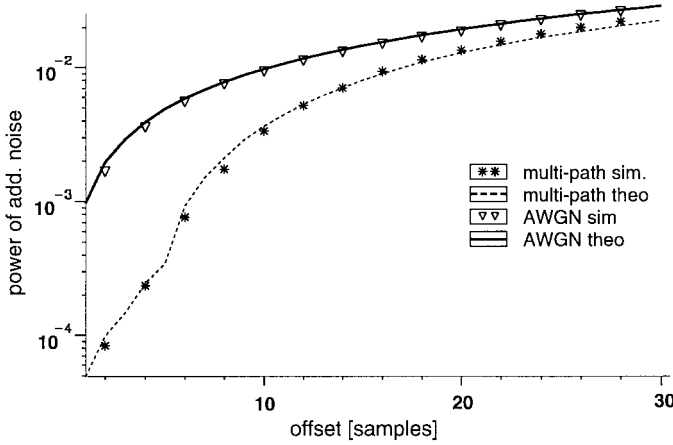
Fig. 3. Power of additional noise caused by a symbol offset. $N = 2048, K = 1705$. Comparison for Gaussian and multipath channel.

The main disturbance, however, is the additional noise $n_{n_\varepsilon; l, k}$ itself. It is well approximated by Gaussian noise with power [1]

$$\sigma_\varepsilon^2 = \sum_i |h_i(t)|^2 \left(2\frac{\Delta\varepsilon_i}{N} - \left(\frac{\Delta\varepsilon_i}{N}\right)^2 \right) \qquad (30)$$

where

$$\Delta\varepsilon_i = \begin{cases} n_\varepsilon - \dfrac{\tau_i}{T}, & n_\varepsilon T > \tau_i \\ \dfrac{\tau_i - T_g}{T} - n_\varepsilon, & 0 < n_\varepsilon T < -(T_g - \tau_i) \\ 0, & \text{else.} \end{cases} \qquad (31)$$

Fig. 3 compares analysis and simulation for two different channels. It can be seen that the power of the additional noise caused by the ISI and ICI strongly depends on the channel profile. Therefore, the absolute value of the symbol offset n_ε is no useful indicator of the required accuracy of symbol timing. Rather, an adequate measure is the loss in system performance due to n_ε [15], [16]. Given a tolerable system degradation of $\Delta\gamma_{\max}$, the following limit on the additional noise power can be derived from (14)

$$\sigma_\varepsilon^2 < \sigma_N^{2\,\text{ideal}} \left(1 - \frac{1}{\Delta\gamma_{\max}} \right). \qquad (32)$$

For instance, an allowable system loss of 0.1 dB calls for σ_ε^2 being 16.4 dB below the channel noise under otherwise ideal synchronization conditions.

In a coherent OFDM system, a timing offset n_ε will have another, possibly even more severe, effect on the performance. According to (11), a timing offset will shift the location of the effective channel "seen" by the receiver. On the other hand, channel estimation requires that the CIR "seen" by the receiver be within a certain estimation window (see Fig. 4) in order to produce an unbiased channel estimate. If, due to a timing offset n_ε, some portions of the effective channel are shifted outside this window, these portions cannot contribute to the estimate. The channel estimate will then suffer an additional
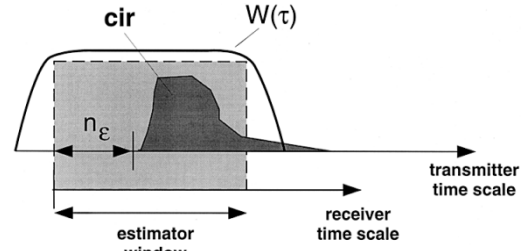

Fig. 4. Channel estimation with timing offset.

error whose variance is given by [15]

$$\sigma_{\text{add}}^2 = E\left\{ \left| \tilde{H}_{l,k}^{n_\varepsilon} - H_{l,k}^\varepsilon \right|^2 \right\} = \frac{K}{N} \sum_i |h_i|^2 |1 - W(\tau_i - \varepsilon T)|^2 \qquad (33)$$

where $W(\tau)$ is the window function used in channel estimation. Due to system performance being very sensitive to errors in the channel estimate, σ_{add}^2 can become significant already for very small portions of the CIR falling outside of the estimation window. Symbol synchronization must therefore be very accurate, particularly when the window $W(\tau)$ is matched very closely to the CIR (the closer the window is matched to the CIR the better the resulting channel estimate).

Note that the above analysis does not only apply to ISI caused by a timing offset but also to ISI caused by a CIR being longer than the guard interval.

C. Effects of Carrier and Sampling Clock Frequency Offsets

OFDM systems, particularly those using small subcarrier bandwidths $1/T_u$, are much more sensitive to frequency offsets than single-carrier systems. This is a nuisance especially in consumer-oriented applications where carrier and sampling frequency oscillators may have sizable offsets. Nevertheless, large offsets are corrected during receiver acquisition (see Part II) so that only small residual offsets need to be considered in the analysis for steady-state operation (tracking mode).

In the presence of a carrier frequency offset Δf and a sampling clock frequency offset $\zeta = (T' - T)/T$, the phase term of (12) becomes

$$\Theta_0(nT') = (1 + \zeta)\Delta f nT. \qquad (34)$$

With the abbreviation $n' = n + N_g + lN_s$, the received samples can be expressed as

$$r_{l,n} = \left(e^{j2\pi n'(1+\zeta)\Delta f T} \right)$$
$$\cdot \left(\sum_i h_i \sum_l \sum_k a_{l,k} \cdot \psi(n'T' - \tau_i) \right) + n_{l,n}$$
$$\psi(n'T' - \tau_i) = e^{j2\pi(k/N)(n'(1+\zeta) - N_g - lN_s - \tau_i/T)}$$
$$\cdot u(n'(1+\zeta)T - lT_s - \tau_i). \qquad (35)$$

1) Effect I—OFDM Symbol Window Drift: From (35), the received samples pertaining to the lth OFDM symbol are seen to fall into a receiver window given by the set of indices n' for which $u(n'[1 + \zeta]T - lT_s - \tau_i) = 1$. Assuming for the moment $\tau_i = 0$, this corresponds to the range

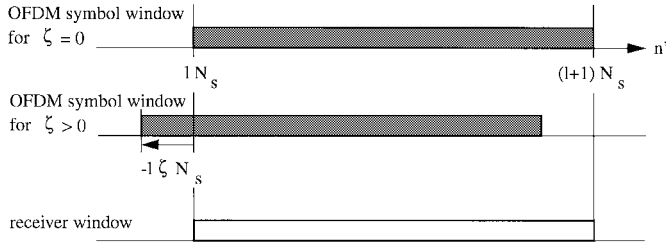$$n' \in [lN_s - \zeta lN_s, \ [l+1]N_s - \zeta[l+1]N_s). \qquad (36)$$

Fig. 5.   OFDM symbol window drift due to sampling clock offset.

Hence, in the absence of sampling clock sync, the transmitted OFDM symbol blocks observed in the receiver window slowly wander away from the ideal observation window $[lN_s, (l + 1)N_s)$. A (positive/negative) sampling clock offset ζ [sampling clock slightly too (slow/fast)] leads to a (left/right) drift of $-\zeta lN_s$ samples. Considering OFDM symbol lengths N_s up to 10^4 and initial sampling clock offsets up to ± 100 ppm ($\zeta = \pm 10^{-4}$), the OFDM symbol window drift, which is visualized in Fig. 5, may well amount to ± 1 sample per OFDM symbol. In the tracking mode where residual offsets are two or three orders of magnitude smaller, OFDM symbol drift is nevertheless a long-term effect (slow random walk), which must be taken care of by the so-called fine timing tracking unit (see Part II).

In the absence of ISI (correct timing sync), demodulating the lth received signal block $\mathbf{r}_l$ via FFT yields

$$z_{l,k} = \left(e^{j\pi\phi_k} \cdot e^{j2\pi((lN_s+N_g)/N)\phi_k} \right) \cdot si(\pi\phi_k)a_{l,k}H_k$$
$$\text{(ICI)} \quad + \sum_{i;\, i\neq k} \left(e^{j\pi\phi_{i,k}} \cdot e^{j2\pi((lN_s+N_g)/(N)\phi_i} \right)$$
$$\cdot si(\pi\phi_{i,k})a_{l,i}H_i + n_{l,k} \tag{37}$$

with cross-subcarrier and subcarrier local frequency offset parameters

$$\phi_{i,k} = (1+\zeta)(\Delta fT_u + i) - k$$
$$\phi_k = \phi_{k,k} \approx \Delta fT_u + \zeta \cdot k \tag{38}$$

respectively. Again modeling the irreducible ICI as additional noise $n_{\Omega;l,k}$, the demodulated signal becomes

$$z_{l,k} = \left(e^{j\pi\phi_k} \cdot e^{j2\pi((lN_s+N_g)/N)\phi_k} \right)$$
$$\cdot \alpha(\phi_k)a_{l,k}H_k + n_{\Omega;l,k} + n_{l,k}. \tag{39}$$

In steady-state tracking mode, the (residual) local offsets ϕ_k are usually small so that the attenuation factor $\alpha(\phi_k) = si(\pi\phi_k)$ is very close to 1 and can therefore be neglected. Likewise, the time-invariant term $e^{j\pi\phi_k}$ cannot be distinguished from the (complex-valued) channel gain factor H_k and may thus be incorporated into H_k. Hence, only the two terms $\exp(j2\pi((lN_s+N_g)/N)\phi_k)$ and $n_{\Omega;l,k}$ remain to be considered.

2) Effect II—Subcarrier Symbol Rotation: From (39), the demodulated symbols are seen to be rotated by a time-variant phasor $\exp(j2\pi((lN_s+N_g)/N)\phi_k)$. From one OFDM symbol to the next, the phase increment is given by the angle $\Delta\varphi_k = 2\pi((N+N_g)/N)\phi_k$, which corresponds to a local subcarrier
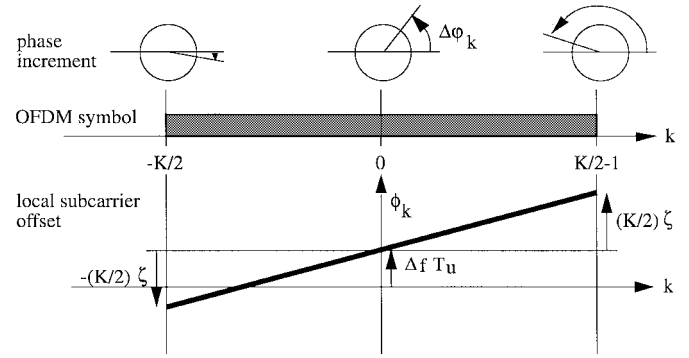

Fig. 6.   Subcarrier symbol rotation due to carrier and sampling frequency offsets.

frequency offset (one OFDM symbol per T_s s) of

$$\frac{\Delta\varphi_k}{2\pi T_s} = \frac{\phi_k}{T_u} = \Delta f + \frac{\zeta}{T_u} \cdot k. \tag{40}$$

While a carrier frequency offset Δf directly translates to the subcarrier level, a sampling clock offset is seen to superimpose an additional offset $(\zeta/T_u)\cdot k$ which is proportional to ζ and the subcarrier index k. Considering again sampling clock offsets up to ± 100 ppm ($\zeta = \pm 10^{-4}$) and $K = 6817$ subcarriers (DVB-T 8k mode standard), this additional offset may be as large as $\pm 0.3408 \cdot (1/T_u)$ at the margins of the OFDM spectrum. The phase increments $\Delta\varphi_k = 2\pi((N+N_g)/N)\phi_k$ and local frequency offsets ϕ_k normalized to subcarrier bandwidth $1/T_u$ are displayed in Fig. 6 for the K subcarriers in the OFDM spectrum. In the tracking mode, subcarrier symbol rotations caused by (residual) local offsets are usually small enough to be tracked by the channel estimator (coherent detection). Also, the linear trajectory of phase increments $\Delta\varphi_k$ versus subcarrier index k (Fig. 6) may be used to track and control residual offsets $\Delta f, \zeta$ (see Part II).

3) Effect III—Frequency Offset Noise (ICI): Analysis of the irreducible ICI noise $n_{\Omega;l,k}$ [(37) and (38)] for small offsets ϕ_k, and under the assumption that channel samples H_k are strongly correlated in frequency direction, yields the approximation to the frequency offset noise power [17]

$$\sigma_{\Omega,k}^2 \approx \frac{\pi^2}{3}|H_k|^2\phi_k^2. \tag{41}$$

As subcarriers which suffer from deep fading do not convey significant information (this is usually counteracted by coding and interleaving across frequency), we may restrict our attention to subcarriers whose channel gain power does not deviate much from the average, i.e., $|H_k|^2 \approx E\{|H_k|^2\} = 1$. Assuming further that all subcarrier offsets ϕ_k are about the same ($\phi_k \approx \Delta fT_u$, only carrier frequency offsets Δf considered), the frequency offset noise power can be approximated by [17]

$$\sigma_\Omega^2 \approx \frac{\pi^2}{3}(\Delta fT_u)^2. \tag{42}$$

This expression is exact in the case of nonselective channels and the absence of a sampling clock frequency offset and a good approximation otherwise.

Given a certain tolerable SNR degradation $\Delta\gamma_{\max}$, the maximum allowable (sub)carrier frequency offset is determined

via (17) as

$$(\Delta f T_u) < \frac{\sqrt{3}}{\pi} \sqrt{\frac{1}{\gamma_{\text{ideal}}} \left(1 - \frac{1}{\Delta\gamma_{\max}}\right)}. \qquad (43)$$

The tolerance against frequency offsets is therefore directly proportional to the subcarrier bandwidth $1/T_u$ and inversely proportional to the square root of the SNR of operation.

As the expression for the frequency noise power σ_{Ω}^2 is similar to that for the fading noise power σ_{fad}^2 (see next Section IV-D), Fig. 7 displays the maximum allowable Doppler frequency f_D versus tolerable SNR loss $\Delta\gamma_{\max}$, which is also valid for carrier frequency offsets by replacing f_D with Δf and scaling the curves down by a factor of $1/\sqrt{2}$.

D. Effect of Time-Selective Fading

In wireless communications, portable and mobile applications are of particular interest. Therefore, $h(\tau, t)$ cannot be assumed to be static. After demodulation via the FFT, the received signal is described by [1]

$$z_{l,k} = a_{l,k} H_{l,k} + n_{l,k} + n_{fad;l,k}. \qquad (44)$$

The CTF $H_{l,k}$ of (8) is now time variant. In the strict sense, $H_{l,k}$ no longer represents the physical channel at a certain time instant but is a complex-valued gain factor resulting from averaging over a time period. Due to the time variance, orthogonality is no longer preserved, causing ICI modeled as additional "fading" noise n_{fad}. Let us assume that each echo path exhibits the (constant) energy $|h_i|^2$ and band-limited fading according to the Jakes Doppler spectrum [18]

$$S(f) = \frac{|h_i|^2}{\pi f_D} \frac{1}{\sqrt{1 - (f/f_D)^2}}, \qquad |f| \le f_D \qquad (45)$$

with Doppler frequency f_D. In [1], the power of the disturbance caused by a single fading multipath component h_i is shown to be given by

$$\sigma_{\text{fad};i}^2 \approx \frac{\pi^2}{6} |h_i|^2 (f_D T_u)^2. \qquad (46)$$

Since the individual channel multipaths can usually be considered uncorrelated, the summation over all power contributions is a good approximation to the resulting total disturbance. Normalizing the (average) total channel energy $\sum_i |h_i|^2$ to unity, the total fading noise power becomes

$$\sigma_{\text{fad}}^2 \approx \frac{\pi^2}{6} (f_D T_u)^2. \qquad (47)$$

Since fading noise is an irreducible receiver disturbance, it may limit the achievable system performance. The tolerance against Doppler is directly proportional to the subcarrier bandwidth $1/T_u$ and inversely proportional to the square root of the SNR of operation. There is a tradeoff involving carrier frequency, mobile speed, transmission bandwidth, and the number of subcarriers. Fig. 7 shows the maximum allowable Doppler frequency versus the maximum system degradation for some SNR operation points ranging between 10–30 dB. In addition to this fading-induced ICI loss, there will be further
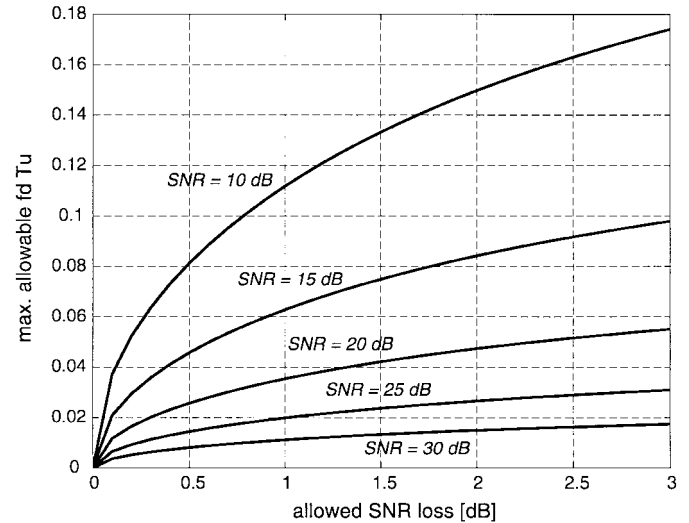

Fig. 7. Doppler versus system degradation. Maximum allowable $f_d T_u$ for a projected allowed system degradation.

degradations through the effects of fading on channel estimation (coherent detection) or differential detection. Hence, the allowable Doppler figures found by analysis [(46), Fig. 7] represent best-case upper bounds.

E. Analog Components

Analog components are very critical in OFDM transmitters and receivers. Main points of concern are the linearity of transmitter amplifiers and the spectral characteristics of receiver radio frequency oscillators, particularly in low-cost consumer applications.

Nonlinear distortions lead to intermodulation of the subcarriers, causing ICI (degrading the OFDM system) as well as out-of-band radiation (degrading adjacent systems) [19], [20]. The latter effect must be prevented already on the transmitter side. Countermeasures such as digital predistortion and the use of a high power backoff are adequate measures to eliminate both effects [21], [22].

Phase noise mainly results from instabilities of the receiver oscillator. These instabilities are characterized by the phase noise spectrum $L_{\phi_N}(f)$ [23]. There are two consequences for the received OFDM signal which may result from a poor phase noise spectrum [24], [25]. First, the loss of orthogonality entails ICI. The power of the ICI component depends on the exact shape of the phase noise spectrum and increases with the number of subcarriers N. An upper bound for the ICI power is given by [24]

$$\sigma_{\text{pn}}^2 \le \sum_{\substack{k=-K/2 \\ k \neq N/2}}^{K/2-1} \int_{-\infty}^{\infty} L_{\phi_N}(f - [f_k - f_{N/2}]) \cdot (si\,(\pi fT))^2 \, df \qquad (48)$$

where $f_k = k/T_u$. Since this effect cannot be compensated with reasonable effort, it sets a minimum requirement for the quality of the oscillator.

A second, less intuitive effect results from the modulation of the drifting phase on the subcarriers, which in [24] has been named common phase error (CPE). As the name suggests,

all subcarriers suffer from the same phase shift. Although the magnitudes of this shift may be quite small, it still can have a significant impact on system performance because this error is correlated (viz. equal) for all symbols modulated onto the subcarriers of an OFDM symbol. Interestingly, the CPE increases as the number of subcarriers N decreases. While the CPE is the same for all subcarriers of the same OFDM symbol, the correlation between CPE's of different OFDM symbols is often too small to be tracked by the channel estimation unit. If necessary, the CPE must therefore be estimated and compensated on a symbol-by-symbol basis [24], [26]. Whether CPE compensation is actually needed depends on the oscillator phase noise mask, the system constellation, and the properties of the outer receiver. System simulations are often the only means of clarifying this issue.

F. Equivalent Signal Model

Equation (49) summarizes the results of the analysis presented above. When compensating the OFDM signal using imperfect parameter estimates, the demodulated subcarrier symbols $\tilde{z}_{l,k}$ are described by

$$\tilde{z}_{l,k} = \alpha(n_{\varepsilon})\, e^{j2\pi(k/N)n_{\varepsilon}} e^{j2\pi l\phi_k((T_u+T_g)/T_u)} a_{l,k}\, H_{l,k}$$
$$+ n_{l,k} + n_{n_{\varepsilon};l,k} + n_{\Omega;l,k} + n_{\text{fad};l,k} + n_{\text{pn};l,k}. \quad (49)$$

Neglecting the (small) attenuation $\alpha(n_{\varepsilon})$, two significant effects remain to be considered:

1) a *phase rotation* that is variant both in time and in frequency;
2) an *additional noise* due to loss of orthogonality (ICI), caused by imperfect symbol timing sync, frequency sync, fading, and phase noise, and due to ISI.

As far as the phase rotations are concerned, they cannot be distinguished from those of the channel and therefore have the same effects. As long as they remain in the same order of magnitude as the frequency- and time-selective characteristics of the channel, they will not further influence performance. Of higher concern is the additional noise. Though for each time instant the individual noise contributions are correlated, analysis shows that their variances can be added if they are small

$$\sigma_{\text{res}}^2 = \sigma_{\varepsilon}^2 + \sigma_{\Omega}^2 + \sigma_{\text{fad}}^2 + \sigma_{\text{pn}}^2. \quad (50)$$

According to our optimization criterion (14), the total variance of the additional noise is required to satisfy

$$\sigma_{\text{res}}^2 < \sigma_N^{2\,\text{ideal}}\left(1 - \frac{1}{\Delta\gamma_{\max}}\right). \quad (51)$$

If coherent modulation is used in addition to the above, a degradation due to the imperfect channel estimation has to be considered.

V. SYNCHRONIZATION OF OFDM SYSTEMS

A. Training Data Format and Synchronization Strategy

An OFDM receiver can extract the information needed for synchronization in two ways as follows.

1) *Before* demodulation of the subcarriers, either from explicit training data [3], [27]–[29] or from the structure
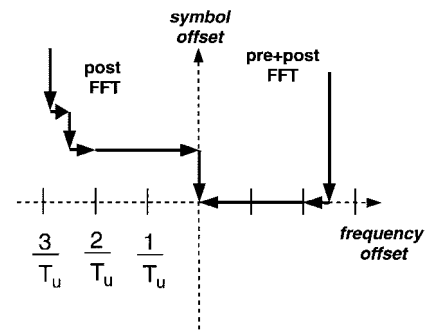

Fig. 8.   Acquisition procedures for systems with and without pre-FFT training data.

of the OFDM signal [30]–[32]. Since no additional training data are needed, the use of the guard interval for synchronization [31], [32] is of particular interest. Unfortunately, the guard interval may naturally be subject to severe ISI so that the performance of such schemes heavily depends on the channel characteristics.

2) *After* demodulation of the subcarriers, the synchronization information can be obtained from training symbols embedded into the regular data symbol pattern [2]. In the past, a variety of algorithms has been proposed for frequency [17], [33]–[35], sampling clock [26], [36], and channel estimation [12], [37]–[40].

The use of post-FFT training data is very effective already for low training data overhead. Unfortunately, using *only* post-FFT training data can significantly prolong system acquisition time. Fig. 8 illustrates the different synchronization procedures for pre- and post-FFT acquisition strategies. At the beginning of the acquisition process, both symbol and frequency offsets may be arbitrarily large. The orthogonality of the signal may therefore be heavily disturbed to an extent where the use of post-FFT training data only allows a coarse synchronization, which must be refined in several iterations. For continual transmission when acquisition time is less critical, this is perfectly tolerable. In the case of burst transmission, however, pre-FFT training data should be provided and used in the receiver in order to rapidly achieve orthogonality *before* the demodulation of the subcarriers. Such schemes allow system acquisition to be completed after one single iteration.

B. Receiver Structure

Fig. 9 shows the basic structure of an OFDM receiver. Depending on the availability of training data, the parameters are estimated before or after demodulation via the FFT. Following downconversion, the received signal should be sampled at a rate $1/T_{\text{samp}} > 1/T$, thus allowing sampling clock synchronization to be performed via interpolation and decimation. After frequency correction and guard interval removal, blocks of N samples pertaining to one OFDM symbol are processed in the FFT. The demodulated subcarrier samples and estimated channel samples (coherent detection) are then passed to an appropriate outer receiver for further processing (equalization, soft bit generation, decoding, deinterleaving, etc.). Note that the proposed structure is free of any feedback loops into the analog part of the receiver. This allows to design
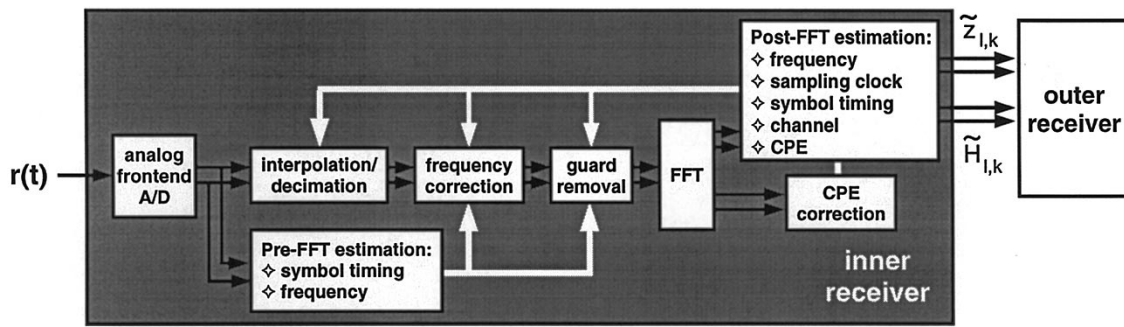
Fig. 9. Structure of an OFDM receiver.

and verify the digital and analog components independently from each other. Given the requirements of the outer receiver and the properties of the analog components, the algorithms for the inner receiver can be systematically developed and optimized as the following.

1) From the characteristics of the target system, the impact of synchronization errors on the performance must be determined. Knowledge of the characteristics of analog components allows to identify critical tasks and the necessary components of the receiver. For example, sampling clock synchronization and CPE correction may or may not be required for the system of interest.
2) If channel estimation is needed, the feasible quality has to be determined. The resulting loss in performance will lead to a smaller $\sigma_N^{2\,\mathrm{ideal}}$, which has to be considered in the further optimization process.
3) Via analysis, the limits for the allowable deviations after correction can be derived. This allows to specify the exact requirements for the different parts of the inner receiver.
4) Taking into account the training format and the specified requirements, receiver algorithms can be designed and optimized. The additional noise due to ICI must be limited to meet (51).

The above methodology allows a concurrent and independent development of the different parts of the receiver while optimizing the overall performance. This is demonstrated in Part II of the paper detailing the receiver design for the European digital terrestrial TV [2] standard.

VI. DISCUSSION AND CONCLUSION

In Part I of the paper, minimum requirements on OFDM synchronization functions have been formulated through the analysis of nonideal transmission conditions and the selection of the SNR loss as the appropriate optimization criterion.

All nonidealities relevant in consumer applications, such as imperfect channel estimation, symbol frame offset, carrier and sampling clock frequency offset, time-selective fading, and critical analog components have been considered, yielding quantitative results as well as valuable insights and also some bounds on maximum allowable imperfections. For example, the bound on Doppler tolerance is important in the design of broad-band OFDM systems intended to be applied in mobile environments.

The effects of relevant imperfections have then been cast into a generalized equivalent system model, which essentially formulates the effect of each nonideality in terms of an additional noise source. This more general model may be used to jointly optimize all synchronization algorithms and find the best compromise between (inner) receiver performance and complexity.

In Part I of the paper, we have focused on steady-state receiver performance in tracking mode, while synchronization strategies for receiver acquisition have only been outlined in the last section. In Part II, all synchronization functions—acquisition and tracking mode alike—will be discussed in detail for the example of a DVB-T receiver.

REFERENCES

[1] F. Claßen, *Systemkomponenten für eine terrestrische digitale mobile Breitbandübertragung*, Ph.D. dissertation, RWTH-Aachen. Aachen, Germany: Shaker Verlag, 1996.
[2] ETSI, "Digital broadcasting systems for television, sound and data services: DRAFT pr ETS 300 744," Mar. 1997.
[3] ETSI, "Radio broadcast systems; digital audio broadcasting (DAB) to mobile, portable and fixed receivers: Final draft pr ETS 300 401," European Telecommunications Standards Institute, Tech. Rep., Nov. 1994.
[4] J. Mikkonen, C. Corrado, and M. Prögler, "Emerging wireless broadband networks," *IEEE Commun. Mag.*, vol. 36, pp. 112–117, Feb. 1998.
[5] J. A. C. Bingham, "Multicarrier modulation for data transmission: An idea whose time has come," *IEEE Commun. Mag.*, vol. 37, pp. 5–14, May 1990.
[6] H. Sari, G. Karam, and I. Jeanclaude, "Transmission techniques for digital terrestrial TV broadcasting," *IEEE Commun. Mag.*, vol. 42, pp. 100–109, Feb. 1995.
[7] T. May, H. Rohling, and V. Engels, "Performance analysis of Viterbi decoding for 64-DAPSK and 64-QAM modulated OFDM signal," *IEEE Trans. Commun.*, vol. 46, pp. 182–190, Feb. 1998.
[8] N. Al-Dhahir and J. Cioffi, "Optimum finite-length equalization for multicarrier transceivers," *IEEE Trans. Commun.*, vol. 44, pp. 56–64, Jan. 1996.
[9] J. Rinne and M. Renfors, "An equalization method for orthogonal frequency division multiplexing systems in channels with multipath propagation, frequency offset and phase noise," in *Proc. IEEE Global Telecommunications Conf. (GLOBECOM)*, Nov. 1996, pp. 1442–1446.
[10] H. Meyr, M. Moeneclaey, and S. Fechtel, *Digital Communication Receivers: Synchronization and Channel Estimation Algorithms*. New York: Wiley, 1997.
[11] L. J. Cimini, "Analysis and simulation of a digital mobile channel using orthogonal frequency division multiplexing," *IEEE Trans. Commun.*, vol. COM-33, pp. 665–675, July 1985.

[12] F. Classen, M. Speth, and H. Meyr, "Channel estimation units for an OFDM system suitable for mobile communications," in *Mobile Kommunikation: ITG-Fachbericht*. München, Berlin Offenbach: VDE-Verlag, Sept. 1995, ITG.

[13] M. Speth and H. Meyr, "Complexity constrained channel estimation for OFDM based transmission over fast fading channels," in *Proc. EPMCC'99*, Mar. 1999, pp. 220–224.

[14] U. Lambrette, *Verfahren zur hochratigen Datenübertragung in Nahbereichsfunknetzen*, Ph.D. dissertation, RWTH-Aachen. Aachen, Germany: Shaker Verlag, 1997.

[15] M. Speth, F. Classen, and H. Meyr, "Frame synchronization of OFDM systems in frequency selective fading channels," in *Proc. IEEE Int. Conf. Vehicular Technology,* 1997, pp. 1807–1811.

[16] U. Lambrette, J. Horstmannshoff, and H. Meyr, "Techniques for frame synchronization on unknown frequency selective channels," in *Proc. IEEE Int. Conf. Vehicular Technology,* May 1997, pp. 1059–1063.

[17] F. Classen and H. Meyr, "Frequency synchronization algorithms for OFDM systems suitable for communications over frequency selective fading channels," in *Proc. IEEE Int. Conf. Vehicular Technology*, Stockholm, Sweden, June 1994, pp. 1655–1659.

[18] J. G. Proakis, *Digital Communications,* 3rd ed. New York: McGraw-Hill, 1995.

[19] C. Rapp, "Effects of the HPA-nonlinearity on a 4-DQPSK/OFDM signal for a digital sound broadcasting system," in *Rec. Conf. ECSC'91 Liege*, Oct. 1991, pp. 179–184.

[20] S. Merchan, A. Armada, and J. Garcia, "OFDM performance in amplifier nonlinearity," *IEEE Trans. Broadcast.*, vol. 44, pp. 106–114, Jan. 1998.

[21] V. Engels and H. Rohling, "Differential modulation techniques for a 34 MBit/s radio channel using OFDM," *Wireless Pers. Commun.*, vol. 2, no. 1/2, pp. 29–44, 1995.

[22] S. Andreoli, H. G. McClure, P. Banelli, and S. Cacopardi, "Digital linearizer for RF amplifiers," *IEEE Trans. Broadcast.*, vol. 43, pp. 12–19, Mar. 1997.

[23] V. Kroupa, "Noise properties of PLL systems," *IEEE Trans. Commun.*, vol. COM-30, pp. 2244–2252, Oct. 1982.

[24] P. Robertson and S. Kaiser, "Analysis of the effects of phase-noise in orthogonal frequency division multiplex (OFDM) systems," in *Proc. ICC'95*, June 1995, pp. 1652–1657.

[25] T. Pollet, M. Van Bladel, and M. Moeneclaey, "BER sensitivity of OFDM systems to carrier frequency offset and Wiener phase noise," *IEEE Trans. Commun.*, vol. 43, pp. 191–193, Apr. 1995.

[26] J. A. C. Bingham, "Method and apparatus for correcting clock and frequency offset, and phase jitter in multicarrier modems," Tech. Rep., Patent 0 453 203 A2, 1992.

[27] T. Keller and L. Hanzo, "Orthogonal frequency division multiplex synchronization techniques For wireless local area networks," in *Proc. IEEE Int. Symp. Personal, Indoor, and Mobile Radio Communications,* 1996, pp. 963–967.

[28] U. Lambrette, M. Speth, and H. Meyr, "OFDM burst frequency synchronization based on single carrier training data," *IEEE Commun. Lett.,* vol. 1, pp. 46–48, Mar. 1997.

[29] T. Schmidl and D. Cox, "Robust frequency and timing synchronization for OFDM," *IEEE Trans. Commun.*, vol. 45, pp. 1613–1621, Dec. 997.

[30] F. Classen and H. Meyr, "Synchronization algorithms for an OFDM system for mobile communication," in *Codierung für Quelle, Kanal und Übertragung: ITG-Fachbericht 130, München*. Berlin Offenbach: VDE-Verlag, Oct. 1994, ITG, pp. 105–114.

[31] F. Daffara and O. Adami, "A novel carrier recovery technique for orthogonal multicarrier systems," *Eur. Trans. Telecommun.*, vol. 8, no. 4, pp. 323–334, July 1996.

[32] J. van de Beek, M. Sandell, and P. Börjesson, "ML estimation of time and frequency offset in OFDM systems," *IEEE Trans. Signal Processing,* vol. 45, pp. 1800–1805, July 1997.

[33] A. Mueller, "Schaetzung der Frequenzabweichung von OFDM-Signalen," in *ITG Fachbericht 124 Mobile Kommunikation,* Sept. 1993, pp. 89–101.

[34] P. Moose, "A technique for orthogonal frequency division multiplexing frequency offset correction," *IEEE Trans. Commun.*, vol. 42, pp. 2908–2914, Oct. 1994.

[35] P. Robertson, "Close-to-optimal one-shot frequency synchronization for OFDM using pilot carriers," in *Proc. IEEE Global Telecommunications Conf. (GLOBECOM)*, 1997, pp. 97–102.

[36] D. C. Cox and T. M. Schmidl, "Low-overhead, low-complexity [burst] synchronization for OFDM," in *Proc. ICC'96,* Dec. 1996.

[37] M. Bossert and A. Donder, "Channel estimation and equalization in orthogonal frequency division multiplexing systems," in *Proc. VDE Conf. 135,* 1995, pp. 485–492.

[38] O. Edfors, M. Sandell, J. van de Beek, S. K. Wilson, and P. Börjesson, "OFDM channel estimation by singular value decomposition," in *Proc. IEEE Int. Conf. Vehicular Technology*, Apr. 1996, vol. 2, pp. 923–927.

[39] Y. Li, L. Cimini, and N. Sollenberger, "Robust channel estimation for OFDM systems with rapid dispersive fading channels," *IEEE Trans. Commun.*, vol. 46, pp. 902–915, July 1998.

Michael Speth (S'99) was born in Munich, Germany, in 1968. He received the Dipl.-Ing. degree in electrical engineering from Aachen University of Technology (RWTH Aachen), Aachen, Germany, in 1995. He is currently heading the group for communication algorithms at the Institute for Integrated Systems in Signal Processing, Aachen University, Aachen, Germany, where he is working toward the Ph.D. degree.

His research interests include digital communications with emphasis on OFDM and algorithm synthesis for synchronization and equalization.

Stefan A. Fechtel (S'89–M'92) was born in Olsberg, Germany, in 1960. He received the Dipl.-Ing. degree in electrical engineering from Aachen University of Technology (RWTH Aachen), the M.Sc. degree from the University of Kansas, Lawrence, Kansas, in 1987, and the Ph.D. degree from Aachen University, Aachen, Germany, in 1993.

From 1993 to 1997, he served as a Postdoctoral Research Engineer and Project Manager at the Institute for Integrated Systems in Signal Processing, Aachen University. Since 1997, he has been with Infineon AG (formerly Siemens AG Semiconductors), Munich, Germany, where he is currently engaged in broad-band digital transceiver research and concept engineering development.

Gunnar Fock was born in Moers, Germany, in 1971. He received the Dipl.-Ing. degree in electrical engineering from Aachen University of Technology (RWTH Aachen), Aachen, Germany, in 1996. Currently, he is a Research Assistant at the Institute for Integrated Systems in Signal Processing, Aachen University, Aachen, Germany, working toward the Ph.D. degree.

His current research interests include digital receiver design with emphasis on synchronization, estimation, and equalization.

Heinrich Meyr (M'75–SM'83–F'86) received the M.S. and Ph.D. degrees from ETH, Zurich, Switzerland.

He spent more than 12 years in various research and management positions in industry before accepting a professorship in electrical engineering at Aachen University of Technology (RWTH Aachen), Aachen, Germany) in 1977. He worked extensively in the areas of communication theory, synchronization, and digital signal processing for the last thirty years. His research has been applied to the design of many industrial products. At RWTH Aachen, he heads an institute involved in the analysis and design of complex signal processing systems for communication applications. He was a cofounder of CADIS GmbH (acquired 1993 by Synopsys, Mountain View, CA) a company which commercialized the tool suite COSSAP, which is extensively used in industry worldwide. He is currently serving on the board of two companies in the communications industry. Recently, he was also appointed as a member of the technical advisory board of MorphICs, Cupertino, CA. Dr. Meyr has published numerous IEEE papers and holds many patents. He is co-author (with Dr. G. Ascheid) of the book *Synchronization in Digital Communications* (New York: Wiley, 1990) and (with Dr. M. Moeneclaey and Dr. S. Fechtel) *Digital Communication Receivers, Synchronization, Channel Estimation, and Signal Processing* (New York: Wiley, 1997). In 1998, he was a visiting scholar at the EE Department at the University of California at Berkeley.

Dr. Meyr has served as a Vice President of International Affairs for the IEEE Communications Society.